JPET Fast Forward. Published on February 18, 2014 as DOI: 10.1124/jpet.113.211714

Clinical and Preclinical Characterization of the Histamine H_4 Receptor Antagonist JNJ 39758979

Robin L. Thurmond, Bin Chen, Paul J. Dunford, Andrew J. Greenspan, Lars Karlsson[1], David La, Peter Ward and Xie L Xu

Janssen Research & Development, L.L.C.

3210 Merryfield Row, San Diego, CA 92121, U.S.A.

JPET Fast Forward. Published on February 18, 2014 as DOI: 10.1124/jpet.113.211714
This article has not been copyedited and formatted. The final version may differ from this version.

Corresponding Author: Robin L. Thurmond
3210 Merryfield Row
San Diego, CA 92121
Phone: 858-784-3108
Email: **rthurmon@its.jnj.com**

Running Title: Pharmacology of JNJ 39758979

Number of text pages: 36

Number of tables: 3

Number of figures: 6

Number of references: 23

Number of words in the

Abstract: 214

Introduction: 401

Discussion: 1210

Abbreviations: H_4R, histamine H_4 receptor; MAD, multiple ascending dose; SAD, single ascending dose; GLP, good laboratory practice; NOAEL, no observed adverse effect level; C_{max}, maximum concentration; $AUC_{0\text{-}24h}$, area under the curve from time 0 to 24 h; T_{max}, time at which maximum plasma concentration is observed; AUC_{last}, area under the curve from time 0 to the last measured time point; V_d/F, volume of distribution

Section: Drug Discovery and Translational Medicine

JPET Fast Forward. Published on February 18, 2014 as DOI: 10.1124/jpet.113.211714
This article has not been copyedited and formatted. The final version may differ from this version.

Abstract

The histamine H_4 receptor (H_4R) has been shown to be involved in both inflammatory and pruritic responses preclinically. JNJ 39758979 is a potent and selective H_4R antagonist with a K_i at the human receptor of 12.5 ± 2.6 nM and greater than 80-fold selectivity over other histamine receptors. The compound also exhibited excellent selectivity versus other targets. JNJ 39758979 showed dose dependent activity in models of asthma and dermatitis consistent with other H_4R antagonists. Preclinical toxicity studies of up to 6 months in rats and 9 months in monkeys indicated an excellent safety profile supporting the clinical testing of the compound. An oral formulation of JNJ 39758979 was studied in a phase 1 human volunteer study to assess safety, pharmacokinetics and pharmacodynamics. The compound was well-tolerated with the exception of dose dependent nausea and no safety issues were noted in the phase 1 study. JNJ 39758979 exhibited good pharmacokinetics upon oral dosing with a plasma half-life of 124-157 h after a single oral dose. In addition, dose dependent inhibition of histamine-induced eosinophil shape change was detected suggesting that the H_4R was inhibited in vivo. In conclusion, JNJ 39758979 is a potent and selective H_4R antagonist that exhibited good preclinical and phase 1 safety in healthy volunteers with evidence of a pharmacodynamics effect in humans.

Introduction

The histamine H_4 receptor (H_4R) has attracted interest as a potential drug target since its discovery in 2000. Preclinical data has suggested a role for the H_4R in a variety of inflammatory diseases. Antagonists of the receptor reduce inflammation and improve lung function in mouse and guinea pig asthma models (Dunford et al., 2006; Cowden et al., 2010a; Somma et al., 2013). Efficacy has also been shown in mouse dermatitis models and a rat model of colitis (Varga et al., 2005; Cowden et al., 2010b; Suwa et al., 2011; Matsushita et al., 2012). Recently, anti-inflammatory activity in mouse arthritis models has been reported with H_4R antagonists (Nent et al., 2013; Cowden et al., 2014). Mice deficient in the H_4R are protected in the asthma, dermatitis and arthritis models further boosting the conclusion that inhibiting the receptor would yield anti-inflammatory effects in humans (Dunford et al., 2006; Cowden et al., 2010b; Cowden et al., 2014). However, the H_4R may not play the same role in all diseases as it appears that neuronal inflammation in experimental autoimmune encephalomyelitis models is exacerbated in H_4R-deficient mice or with treatment with an H_4R antagonist (del Rio et al., 2012; Ballerini et al., 2013). In addition to a role in inflammation, the receptor also appears to control pruritus in numerous preclinical models of itch (Dunford et al., 2007; Yamaura et al., 2009; Rossbach et al., 2011; Ohsawa and Hirasawa, 2012; Shin et al., 2012). This data along with the anti-inflammatory data in dermatitis models suggests that H_4R antagonists may be useful in the treatment of atopic dermatitis.

Preclinical data with H_4R receptor antagonists have generated interest in exploring the use of such antagonists in humans. To date, limited clinical data on H_4R antagonists has been reported. Data from phase 1 studies with two H_4R antagonists, UR-63325 and PF-3893787, have been reported at scientific meetings and are summarized in a review by Salcedo et al. (Salcedo et

al., 2013). UR-63325 was reported to have been studied in both single dose and multiple doses in healthy volunteers with no significant safety issues. The compound was also shown to have a pharmacodynamics effect in inhibiting the histamine-induced shape change in eosinophils ex vivo. Similar findings were reported with PF-03893787 ((R)-N4-(cyclopropylmethyl)-6-(3-(methylamino)pyrrolidin-1-yl)pyrimidine-2,4-diamine), another H_4R antagonist (Mowbray et al., 2011). In the current work the detailed phase 1 clinical safety, pharmacokinetic and pharmacodynamics data with the selective H_4R antagonist, JNJ 39758979, are presented.

JPET Fast Forward. Published on February 18, 2014 as DOI: 10.1124/jpet.113.211714
This article has not been copyedited and formatted. The final version may differ from this version.

Materials and Methods

Materials. JNJ 39758979 ((*R*)- 4-(3-Amino-pyrrolidin-1-yl)-6-isopropyl-pyrimidin-2-ylamine; Figure 1) was synthesized as previously described (Savall et al., 2014).

Pharmacology. Binding and functional assays for the various histamine receptors were carried out as previously described (Thurmond et al., 2004; Yu et al., 2010). Muscarinic receptor binding assays were carried out with cell membranes from CHO cells transfected with human M_1, M_2, M_3, and M_4 receptors. The radioligand used was 0.2 nM [^{3}H]N-methyl scopolamine and nonspecific binding was defined with 1 μM unlabeled atropine. A panel of 50 different biogenic amine receptors, neuropeptide receptors, ion channel binding sites, and neurotransmitter transporter binding assays was run by Cerep, Inc. (Redmond, WA). The full methods and references can be found on the Cerep website (www.cerep.fr). The assays were run at 1 μM of JNJ 39758979. The kinase selectivity was determined with the KinaseProfiler™ panel (Gao et al., 2013) and was run by EMD Millipore Corp. (San Diego, CA). Histamine-induced eosinophil shape change was conducted as previously described (Ling et al., 2004; Yu et al., 2010). For the whole blood assay, one set of samples were untreated and not manipulated before measurement. Others were processed as previously described, but in the absence of histamine (baseline) as the processing itself leads to some level of eosinophil activation. The final set of samples where processed and treated with histamine with or without JNJ 39758979. Statistical analysis for the eosinophil shape change data was carried out with a Student's t-test for all statistical comparisons between two groups and a one-way ANOVA with post-hoc Dunnett's test for comparison of three or more groups. The ovalbumin mouse asthma model and the fluorescein isothiocyanate-induced mouse dermatitis model were conducted as previously described

(Dunford et al., 2006; Cowden et al., 2010b). JNJ 39758979 was dosed orally in 20% hydroxypropyl-β−cyclodextrin. For the asthma model the compound was administered 20 min prior to the daily allergen challenge. In the fluorescein isothiocyanate model the compound was given 30 minutes before and 4 hours after fluorescein isothiocyanate application to the ear. Statistical analysis was carried out with a one-way ANOVA with post-hoc Dunnett's test.

Toxicology Studies. JNJ 39758979 was evaluated in repeat-dose toxicity studies for up to 6 months duration in Sprague-Dawley rats and 9 months in cynomolgus monkeys. Studies in rats were conducted with the following doses and study duration: 0, 10, 50, 300 mg/kg/day (N=10/sex/group) for 1 month; 0, 10, 50, 250 mg/kg/day (N=10/sex/group) for 3 months; 0, 25, 50, 100, 200 mg/kg/day (N=20/sex/group) for 6 months. Studies in monkeys were conducted with the following doses and study duration: 0, 6, 20, 60 mg/kg/day (N=3/sex/group) for 1 month; 0, 2, 6, 30 mg/kg/day (N=4/sex/group) for 3 months; 0, 3, 10, 30 mg/kg/day (N=4/sex/group) for 9 months. JNJ 39758979 was formulated in water and administered daily by gavage. Rats and monkeys were examined for mortality, clinical signs, ophthalmoscopic changes, body weight, food consumption, hematology, clinical chemistry, anatomic pathology, and toxicokinetics. In addition, monkeys were examined for electrocardiographic changes. Rats and monkeys were also assessed for reversal of any effects following a 1 month recovery period. These studies were conducted in compliance with good laboratory practice (GLP) regulations.

Clinical Study. This was a single-center, double-blind, randomized, placebo-controlled study in healthy male and female subjects of non-childbearing potential (postmenopausal or otherwise sterile). The study was conducted in Belgium from Sept. 2008-June 2009. JNJ

39758979 was supplied as a powder for reconstitution with sterile water to provide oral solutions of 5 mg/mL and 100 mg/mL. In the single ascending dose (SAD) portion of the study, eligible male subjects in each treatment group were randomized to receive either a single oral dose of JNJ 39758979 (n=6) or placebo (n=3), after an overnight fast. Dose levels for the different groups were 10, 30 (n=5 only), 100, 300, 600 and 1200 mg of JNJ 39758979. The doses of JNJ 39758979 were escalated in a stepwise fashion if the safety, tolerability and plasma pharmacokinetic profile (up to 24 hours) were deemed acceptable. In the multiple ascending dose (MAD) part of the study, male subjects received oral doses of placebo or 30, 100 (n=5 only), 300, and 600 mg (300 mg twice daily) of JNJ 39758979 for 14 consecutive days. The doses were escalated in a stepwise fashion if the safety, tolerability and plasma pharmacokinetic profile were deemed acceptable. In addition female subjects were dosed with either 300 mg of JNJ 39758979 (n=6) or placebo (n=3) for 14 consecutive days. There were no early withdraws in the SAD part of the study, however in the MAD portion of the study two placebo patients discontinued early. The main criteria for inclusion in the study were healthy male and postmenopausal or non-childbearing (i.e. surgically sterile) female subjects between 18 and 55 years of age, inclusive; body mass index within 18 to 29 kg/m^2, with a minimum body weight of 50 kg; supine blood pressure (after resting for 5 minutes) between the range of 90 to 139 mm Hg systolic and 50 to 89 mm Hg diastolic, inclusive. For all parts of the study, adverse events and concomitant medications were assessed and recorded from screening through follow-up. The following safety measures were assessed at various timepoints during the study: medical history, physical examination, neurological examination, 12-lead electrocardiogram (ECG), continuous ECG monitoring (telemetry), vital signs (blood pressure, heart rate, respiratory rate, and temperature), clinical laboratory tests including blood chemistry, hematology, coagulation, and serology tests

(hepatitis B surface antigen, hepatitis C virus antibody, and human immunodeficiency virus antibody), urinalysis, alcohol analysis, urine pregnancy test (females), serum pregnancy test (females), urine drug screen, 24-hour urine for creatinine clearance, protein, and albumin excretion rate, and spot urine albumin/creatinine ratio.

Pharmacokinetic Evaluation. For all parts of the clinical study, venous blood samples were taken for the measurement of JNJ 39758979 plasma concentrations. A validated, specific, and sensitive liquid chromatography-mass spectrometry/mass spectrometry method was used for analysis of plasma samples to determine concentrations of JNJ 39758979. A high-performance liquid chromatographic-triple quadrupole mass spectrometric (LC-MS/MS) method for the quantitation of JNJ 39758979 in human plasma with K_2EDTA anticoagulant and a protein precipitation extraction procedure over a concentration range of 2 to 500 ng/mL. The analytical reference standard of JNJ 39758979 and an internal standard were used to quantitate JNJ 39758979 in these plasma samples. Pharmacokinetic parameters were determined from plasma data of JNJ 39758979 after single oral administration or after multiple oral administrations. Data obtained from placebo subjects was not included in the PK analysis as all plasma concentration data obtained for these subjects were below the lower limit of quantification (2 ng/mL). Due to insufficient numbers of timepoints with concentrations above the lower limit of quantification in some cohorts of the SAD portion of the study, only the maximum concentration (C_{max}) and time of maximum concentration (T_{max}) were reported for subjects in the 10 mg treatment group while C_{max}, T_{max}, area under the curve from time 0 to 24 h (AUC_{0-24}), and the area under the curve from time 0 to the last measured time point (AUC_{last}) were reported for the 30 mg treatment group.

JPET Fast Forward. Published on February 18, 2014 as DOI: 10.1124/jpet.113.211714
This article has not been copyedited and formatted. The final version may differ from this version.

Pharmacodynamic assay. Venous blood samples were collected into potassium EDTA tubes at the timepoints specified. The collected blood volumes were 4.9 mL. To measure histamine induced eosinophil shape change, 1 mL of blood was treated with 0 or 0.3 μM of histamine in the presence of 3 μM ranitidine for 10 minutes at 37^{o}C. Each treatment was done in duplicate. Following the histamine stimulation, the blood was fixed and the shape change of eosinophils was measured by gated autofluorescence forward scatter assay on a Bayer Advia 120 clinical hematology analyzer. Two scans were acquired for each replicate. Repeated scans were summarized by calculating the average of the means of the forward scatter. Sample replicates were summarized by calculating the average of the scan replicates. The eosinophil population was gated by high peroxidase staining and low forward scatter, based on positive and negative controls provided by the Advia 120 manufacturer. To evaluate the effect of compound on eosinophil forward scatter upon histamine stimulation, the variable '% Change' was calculated as: (Mean $Scatter_h$ - Mean $Scatter_b$) / Mean $Scatter_b$ x 100, where Mean $Scatter_h$ denotes the mean scatter of eosinophil treated with 0.3 μM of histamine and Mean $Scatter_b$ denotes the mean scatter of eosinophils treated with control (no histamine). Statistical analysis was carried out using a one-way ANOVA with post-hoc Dunnett's test.

In addition to histamine-induced eosinophil shape change, serum was collected in the MAD portion of the study pre-dose on days 1, 2, 7 and 14 as well as 4 h post-dose on day 1. Serum markers were measured with a multiplex ELISA assay: TruCulture™ MAP, Antigen Map v1.6 (Rules- Based Medicine, Austin, TX). MAP assays were performed at Rules-Based Medicine (Austin, TX). For each assay in Rules Based Medicine MAP, values below the detection limit were replaced with the lowest value in the given assay, or the least detectable

dose of the assay, whichever is smaller. The least detectable dose was determined as the mean plus 3 times the standard deviation of 20 blank readings.

JPET Fast Forward. Published on February 18, 2014 as DOI: 10.1124/jpet.113.211714
This article has not been copyedited and formatted. The final version may differ from this version.

Results

In vitro Pharmacology. The pharmacological activity of JNJ 39758979 at the histamine H_1, H_2, H_3 and H_4 receptors of various species was investigated in vitro. JNJ 39758979 has a high affinity for the human H_4R with a K_i value of 12.5 ± 2.6 nM (Table 1). The compound did not display agonist activity in the systems tested up to concentrations of 10 μM and in fact displayed properties of a competitive antagonist of histamine with a pA_2 value of 7.9 ± 0.1. JNJ 39758979 exhibits high affinity for the mouse and monkey H_4R with less affinity for the rat, guinea pig and dog receptors. The compound was a competitive antagonist at the mouse, rat and monkey receptors with no agonist activity detected. The compound is a weak ligand for the human H_3 receptor and has modest affinity for the mouse and rat H_3 receptor. For the human and mouse there is a good separation between H_4R and H_3 receptor affinity, however for the rat the affinity is similar. There is little, if any, affinity for the H_1 and H_2 receptors.

JNJ 39758979 was evaluated for selectivity against other non-histamine receptor targets. These targets represent major classes of biogenic amine receptors, neuropeptide receptors, ion channel binding sites, and neurotransmitter transporters. There was less than 20% inhibition at 1 μM for all of the targets, except for a 64% inhibition detected for the muscarinic M_3 receptor (Supplemental Table S1). Since this initial assay was a screening assay, the inhibition of the human muscarinic receptors was followed up by more definitive detailed determination of the K_i values in transfected cells. JNJ 39758979 had no affinity up to 10 μM against the human muscarinic M1, M2, M3 or M4 receptors. The difference in M3 results between the inhibition assay and the K_i determination assay is most likely accounted for by the single concentration analyzed in the inhibition assay and the fact that this is a high throughput format. JNJ 39758979

was also tested at 10 μM against 66 kinases and did not show greater than 25% inhibition for any of the kinases tested (Supplemental Table S2).

The pharmacological activity of JNJ 39758979 on the human eosinophil histamine-induced shape change was investigated in vitro. Histamine is able to induce chemotaxis of eosinophils and this can be represented by a change in cell shape (Ling et al., 2004). Increasing concentrations of JNJ 39758979 caused a rightward shift in the histamine dose-response for inducing eosinophil shape change indicating that the compound was behaving as an antagonist (Figure 2A). The assay cannot be conducted under equilibrium conditions since the reaction occurs within minutes of adding the agonist, and therefore, it is not possible to derive meaningful IC_{50} or K_i values (Ling et al., 2004). When tested in whole blood, JNJ 39758979 caused a dose-dependent inhibition on histamine-induced eosinophil shape change (Figure 2B). In both cases significant inhibition of eosinophil shape change was observed at concentrations equal to or greater than 100 nM (22 ng/ml). JNJ 39758979 also inhibited the histamine induced mouse bone marrow derived mast cell chemotaxis with an IC_{50} of 8 nM when 10 μM histamine was used. An estimation of the K_i can be made using the Cheng-Prusoff equation given an EC_{50} for histamine of 10 μM. This yields an apparent K_i of 4 nM consistent with the results from the mouse-binding assay (5 nM).

In vivo Pharmacology. Previously it had been shown that the H_4R mediates inflammation in an murine asthma model (Dunford et al., 2006) and therefore effects of JNJ 39758979 were investigated in this model. In ovalbumin-sensitized mice, different doses of JNJ 39758979 were administered orally before each of the daily challenges of ovalbumin. Under these conditions, JNJ 39758979 showed dose-related inhibition of cellular inflammation induced by ovalbumin challenge compared with vehicle-treated animals (Figure 3A). A significant reduction of

eosinophils in lavage fluid was observed at 0.2 mg/kg doses and higher compared to vehicle treatment animals. There was no statistical significant difference between any of the dose groups. There was a trend for inhibition of total cells and lymphocytes, but this did not reach statistical significance. No changes in macrophages or neutrophils were observed. The effect of JNJ 7777120 is shown for comparison and was similar to that previously reported (Dunford et al., 2006). The C_{max} of the compound at 0.2 mg/kg based on previously published pharmacokinetic studies was estimated to be approximately 32 to 50 nM (7-11 ng/mL)(Savall et al., 2014). These findings suggest that JNJ 39758979 affects inflammatory infiltrates in a model of allergic airway inflammation and may have therapeutic utility in allergic lung disease.

The effects of JNJ 39758979 in a murine model of Th2-dependent contact hypersensitivity have also been investigated. Dermal administration of fluorescein isothiocyanate to sensitized animals resulted in inflammatory edema. Treatment with JNJ 39758979 at doses of 20 and 50 mg/kg twice a day significantly reduced the change in ear edema (Figure 3B). Data with JNJ 28307474 is shown for comparison and is similar to that previously reported (Cowden et al., 2010b). These data suggest that JNJ 39758979 may be useful in the treatment of Th_2-dependent skin diseases, such as atopic dermatitis.

Toxicology. The preclinical pharmacology of JNJ 3975897 suggested that it was a good candidate for clinical development. To support this, preclinical toxicology studies were carried out. JNJ 39758979 was evaluated in repeat-dose toxicity studies of up to 6 months duration in rats and 9 months in monkeys. In the GLP 3-month oral toxicity study in rats (0, 10, 50, and 250 mg/kg/day), the no observed adverse effect level (NOAEL) was 50 mg/kg/day (915 and 1290 ng/mL C_{max}, and 5980 and 8490 ng•h/mL $AUC_{0\text{-}24h}$ in males and females, respectively). At 250 mg/kg/day (5390 and 5940 ng/mL C_{max} and 66,500 and 79,200 ng•h/mL $AUC_{0\text{-}24h}$ in males and

JPET Fast Forward. Published on February 18, 2014 as DOI: 10.1124/jpet.113.211714
This article has not been copyedited and formatted. The final version may differ from this version.

females, respectively), findings included decreased body weight, slightly increased alanine aminotransferase, aspartate aminotransferase, and alkaline phosphatase, and subacute inflammation and foamy macrophages in the lung. The foamy macrophages correlated ultrastructurally to intralysosomal lamellar bodies consistent with phospholipidosis. There was no evidence of significant hematologic, bone marrow, or lymphoid organ changes. All changes showed partial to full reversal after a 1-month recovery period. In the GLP 6-month toxicity study (doses of 0, 25, 50, 100, and 200 mg/kg/day), clinical pathology findings and the occurrence of foamy macrophages in the lung were similar to that in the 3-month study. The NOAEL in the 6-month study was 100 mg/kg/day for males (2120 ng/mL C_{max}, 17600 ng•h/mL $AUC_{0\text{-}24h}$) and 200 mg/kg/day for females (4460 ng/mL C_{max}, 49,400 ng•h/mL $AUC_{0\text{-}24h}$).

In GLP oral gavage toxicity studies in monkeys, JNJ 39758979 was administered at doses up to 30 mg/kg/day for 3 months (0, 2, 6, and 30 mg/kg/day) and 9 months (0, 3, 10, and 30 mg/kg/day). No compound-related adverse effects were observed in males at any dose or duration or in females at any dose for 3 months. Females dosed at 30 mg/kg/day for 9 months had decreased body weight. There was no evidence of significant hematological or bone marrow abnormalities in either study. In particular there were no meaningful differences between bone marrow cytology in the monkeys administered test article at 30 mg/kg/day for 3 months compared to concurrent controls. The NOAEL in male monkeys was the high dose of 30 mg/kg/day for both 3 and 9-month administration (C_{max} 1,470 and 1,390 ng/mL and $AUC_{0\text{-}24}$ 21,600 and 17,400 ng•h/mL, respectively). The NOAEL in female monkeys was 30 mg/kg/day for 3-month administration (C_{max} 1,560 ng/mL and $AUC_{0\text{-}24}$ 21,200 ng•h/mL) and 10 mg/kg/day for 9-month administration (C_{max} 574 ng/mL and $AUC_{0\text{-}24}$ 5,920 ng•h/mL).

JPET Fast Forward. Published on February 18, 2014 as DOI: 10.1124/jpet.113.211714
This article has not been copyedited and formatted. The final version may differ from this version.

In both rats and monkeys, there was no evidence of immunotoxicity based on the absence of effects on hematology (Supplemental Table S6, S7), bone marrow cytology (Supplemental Table S8), and lymphoid organs (Supplemental Table S9, S10). The toxicology data with JNJ 39758979 indicate that there are no significant safety issues related to the inhibition of the H_4R. To further confirm this, studies were carried out to compare C57BL/6 wild-type to H_4R-deficient mice. Mice were compared at approximately 7 weeks of age as well as 30-43 weeks old. Five females and five males were used in each group. There were no consistent differences in bone marrow cytology between the wild-type and H_4R-deficient mice at either juvenile or mature phases (Supplemental Table S11, S12, S13).

Human Clinical Studies. The preclinical toxicology profile was supportive of further investigation in clinical studies. This, combined with the pharmacology data indicating potential benefit in the treatment of a variety of inflammatory diseases, prompted the initiation of a clinical study to evaluate the safety, tolerability, pharmacokinetics, and pharmacodynamics of single and multiple ascending oral doses of JNJ 39758979 in healthy subjects. The study was conducted at a single site in Belgium from Sept. 2008-June 2009.

The single-dose JNJ 39758979 pharmacokinetic characteristics were evaluated at doses ranging from 10 to 1200 mg with a 5 or 100 mg/mL oral solution under fasting conditions in healthy subjects (Figure 4 and Supplemental Table S3). JNJ 39758979 was rapidly absorbed into plasma (median T_{max} of 0.5 to 2 hours). Both C_{max} and AUC_{last} in plasma were slightly more than dose proportional between the doses of 30 and 600 mg, but less than dose proportional between the doses of 600 and 1200 mg. The large apparent volume of distribution (V_d/F) indicates extensive tissue distribution of JNJ 39758979. The elimination of JNJ 39758979 appeared to be multiphasic with the mean terminal $t_{1/2}$ ranging from 126 to 157 hours.

JPET Fast Forward. Published on February 18, 2014 as DOI: 10.1124/jpet.113.211714
This article has not been copyedited and formatted. The final version may differ from this version.

In healthy subjects, the multiple-dose pharmacokinetic characteristics of JNJ 39758979 were evaluated at doses ranging from 30 mg q.d. to 300 mg b.i.d. for 14 days using an oral solution under fasted conditions (Figure 5 and Supplemental Table S4). JNJ 39758979 was rapidly absorbed into the systemic circulation after multiple oral doses with a median T_{max} of 0.5 to 2 hours. Both C_{max} and AUC_{0-24} (Days 1 and 14) were increased more than dose proportionally between the doses of 30 and 100 mg q.d., and 100 and 300 mg q.d. Following multiple oral doses of 300 mg b.i.d. for 14 consecutive days, AUC within 24 hours was approximately 100% greater than that for the 300 mg q.d. on both Days 1 and 14. JNJ 39758979 plasma concentrations appeared to reach steady state by Day 14 for all dose levels and regimens evaluated. The accumulation ratio based on AUC_{0-24h} observed on Day 1 and Day 14 was 3 to 4, corresponding to an effective $t_{1/2}$ approximately ranging from 40 to 60 hours. At the dose of 300 mg q.d., steady state C_{max} and AUC_{0-24h} values in healthy female subjects were approximately 20% and 60% greater than those in healthy male subjects, respectively. The mean fluctuation index of JNJ 39758979 was low ranging from 0.852 to 2.60, suggesting a good maintenance of plasma levels of JNJ 39758979 over time. The elimination of JNJ 39758979 appeared to be multiphasic with the mean terminal $t_{1/2}$ ranging from 134 to 296 hours on Day 14 across the doses studied. JNJ 39758979 was detectable in plasma up to 56 days after the last dose on Day 14.

Clinical Safety. At single doses ranging from 10 to 1200 mg JNJ 39758979, the only safety and tolerability issues identified were related to gastrointestinal adverse events. No deaths, serious adverse events, discontinuations due to adverse events, or other significant adverse events occurred. Overall, 20 of 35 (57%) subjects in the single-ascending dose study reported 1 or more adverse events within 7 days of dosing with JNJ 39758979. The most frequently

reported adverse events were diarrhea, nausea, headache, abdominal pain and vomiting (Table 2). No other consistent, dose-related adverse events were observed. Most events were mild, were self-limited, and occurred in a dose-dependent fashion. No clear or consistent treatment-related changes were observed in vital signs, ECG parameters, mean serum hematology, chemistry, coagulation, urinalysis, or urine microscopy parameters.

Overall, no additional safety issues were identified after multiple oral doses (30 to 300 mg once daily and 300 mg b.i.d.) of JNJ 39758979 for up to 14 days. There were no deaths, serious adverse events, discontinuations due to adverse events, or other significant adverse events reported in subjects given JNJ 39758979. Multiple oral doses of JNJ 39758979 ranging from 30 mg to 600 mg (300 mg b.i.d.) for up to 14 days were safe. The most consistent adverse events of note were gastrointestinal adverse events, chiefly nausea and abnormal feces (Table 3). Headaches also occurred frequently, but at generally similar rates to placebo. Adverse events are summarized up to 7 days after the last dose of JNJ 39758979. No adverse events of insomnia or somnolence were reported even though JNJ 39758979 does cross the blood-brain barrier. This is in contrast with what is reported with central nervous system-penetrant H_1 or H_3 receptor antagonists. No clear or consistent treatment-related changes were observed in vital signs, ECG parameters, mean serum hematology, chemistry, coagulation, urinalysis, or urine microscopy parameters. Of particular note there was no mean change from baseline absolute neutrophil count following administration of multiple doses of JNJ 39758979 over 14 days at doses up to 300 mg b.i.d.

Human Pharmacodynamics. Histamine-induced eosinophil shape change was used as a pharmacodynamic readout in the Phase 1 study. At baseline (24 h prior to the first dose) all treatment groups in both the SAD and MAD portion of the study had a similar percentage change

in mean forward scatter upon histamine stimulation, with the exception of the 10 mg single dose group, which had a mean forward scatter that was statistically higher than those in the placebo group (Figure 6A, B). For the SAD cohorts the original planned sampling time points were 3, 6 and 24 h after the dose. However, a review of the pharmacokinetic data from earlier cohorts indicated that the T_{max} for the compound occurred earlier than 3 hours following dosing. Therefore, starting with the 300 mg cohort, samples were collected at 0.75 h, 6 and 24h after dosing. There was no significant inhibition of the histamine-induced shape change at any time point for the 10, 30 and 100 mg cohorts relative to placebo, although the 100 mg cohort showed a trend for inhibition at 6 h. It should be noted that for these cohorts the effect at the T_{max} for the drug as not assessed. For the 300 mg, 600 mg and 1200 mg significant inhibition of the histamine-induced shape change compared to the placebo group occurred at 0.75 and 6 h. The mean inhibition ranged from 60-100%. Inhibition at 24 h was also noted for these dose groups, but only data from the 600 and 1200 mg cohort reached statistical significance.

For the MAD portion of the study, samples were collected 1 day prior to dosing on Day 1 and on day 14 (0.75, 6, 24, 48h post dose). No inhibition was seen at any time point in the 30 mg group (Figure 6B). Statistically significant histamine-induced shape change inhibition was observed in the 100, 300 and 300 mg b.i.d. cohorts at 0.75h (around T_{max}) on the last day of dosing (Day 14). The mean inhibition was approximately 75-100%. Inhibition as observed at 6 and 24h post dose of day 14 for the 300 mg and 300 mg b.i.d. groups, but the data for the 300 mg groups did not reach statistical significance at 6 h. At 24 hours post Day 14 dose, 81.7% inhibition was observed in the 300 mg cohort. In general the data from the 300 mg female cohort was similar to 300 mg male cohort at all time points.

JPET Fast Forward. Published on February 18, 2014 as DOI: 10.1124/jpet.113.211714
This article has not been copyedited and formatted. The final version may differ from this version.

A panel of 98 serum proteins was analyzed in the MAD portion of the study from serum collected pre-dose on days 1, 2, 7 and 14 as well as 4 h post-dose on day 1. No changes were detected upon treatment with JNJ 39758979, although 22 proteins were below the limit of quantification. A list of the proteins tested is included in Supplemental Table S5.

JPET Fast Forward. Published on February 18, 2014 as DOI: 10.1124/jpet.113.211714
This article has not been copyedited and formatted. The final version may differ from this version.

Discussion

Since its discovery in 2000 it has been suggested that the H_4R is an attractive target for the development of therapies for the treatment of a variety of diseases. Here we describe the preclinical and clinical characterization of one of the first H_4R antagonists to enter the clinic. The clinical data reported here was from a phase 1 study conducted in 2008-2009.

JNJ 39758979 binds to the human H_4R with a high affinity and has good selectivity over other histamine receptors. As for many of the other H_4R ligands, JNJ 39758979 does display differences at the H_4R across the various species. In particular, while the compound has a high affinity for the human, mouse and monkey receptor, it has low affinity for the rat and dog receptor. The high affinity at the mouse receptor is important for the preclinical in vivo characterization of the compound, but the low affinity in rat and dog impacted the choice of toxicology species. In addition the compound is an antagonist at the H_4R in all species and does not display any agonist activity. This consistent pharmacology across species is crucial when interpreting preclinical efficacy and toxicology data.

The activity of JNJ 39758979 in vivo was consistent with previous reports of other H_4R antagonist in these models (Dunford et al., 2006; Cowden et al., 2010b). Dose dependent inhibition of eosinophil influx in a mouse asthma model and ear edema in a mouse dermatitis model was observed. For the asthma model effects were seen starting at doses of 0.2 mg/kg and the C_{max} for the compound at this dose was estimated to be 32 to 50 nM (7-11 ng/mL). This is about ten times higher than the measured K_i for the mouse H_4R (5 nM). Efficacy in the dermatitis model was seen with doses that gave trough concentrations that were around three-fold higher than C_{max} in the asthma model (170 nM; 38 ng/mL). Experience with a variety of H_4R antagonists in these models suggest that the C_{max} is the most important parameter driving

efficacy in the mouse asthma model, whereas trough concentrations were most important in the dermatitis model. This is most likely due to the transient exposure experienced to the aerosolized antigen in the asthma model compared to the hapten in the dermatitis model. These data suggest that targeting trough concentration of JNJ 39758979 values of 10-40 ng/ml would be necessary for efficacy in humans. The efficacy data in these models combined with that previous reported in pruritus and arthritis models (Savall et al., 2014) indicate that the compound could have utility in the treatment of a variety of inflammatory diseases.

JNJ 39738979 was able to inhibit histamine-induced eosinophil shape change in vitro. A statistically significant inhibition was observed starting at 100 nM (~20 ng/ml). This pharmacodynamic marker was also used in the phase 1 clinical study. Inhibition of the shape change was detected indicating that JNJ 39758979 was able to block the H_4R in humans. In general inhibition was seen at doses and time points where the plasma concentration was above 20 ng/ml, which is consistent with the in vitro results. This pharmacodynamic assay cannot be performed in mice due to the low numbers of circulating eosinophils and their lack of autofluorescence, however given the similarity in potency at the human and mouse receptor one may also expect that plasma concentrations above 20 ng/ml would yield an effect in the mouse. This concentration range is within that predicted from the preclinical efficacy results (10-40 ng/ml) and once again supports this range as being necessary for efficacy in humans. However, this relationship may not hold for every compound since it will depend on the degree of protein binding and tissue distribution. Compounds that are highly protein bound and/or highly distributed to tissues may require higher plasma concentrations to show efficacy in such a pharmacodynamic marker. Nevertheless, for JNJ 39758979 the pharmacokinetic data in combination with the pharmacodynamic data suggest that daily dosing at 100 mg or above would

achieve the predicted efficacious steady state trough plasma levels and would yield target engagement.

JNJ 39758979 was absorbed with a median T_{max} of 0.5 to 2 hours. The disposition was triphasic with a mean terminal elimination $t_{1/2}$ ranging from 126 to 157 hours across the dose range between 100 to 1200 mg. Reasons for the slow elimination are unknown. Foamy alveolar macrophages consistent with phosopholipidosis were observed in rats following large doses of JNJ 39758979. Compounds inducing phospholipidosis are known to accumulate in cells in association with the increased phospholipids (Reasor et al 2006). However, it is unlikely that the slow elimination is due to phospholipidosis as the long half-life was observed at doses and exposures below those associated with phospholipidosis, but the contribution of lysosomal trapping on slow drug elimination cannot be ruled out.

JNJ 39758979 PK variability was moderate to high, ranging from 31% to 50% for C_{max} and 36% to 53% for AUC_{inf} after single-dose administration while its variability appeared to be lower at steady state, ranging 7% to 33% for $C_{max,ss}$ and 9% to 24% for $AUC_{0-24,ss}$. Formal statistical analysis on dose proportionality was not done due to limited sample size and high variability. However, both C_{max} and AUC for JNJ 39758979 increased with the increase of dose after single- and multiple-dose administration. The increase of C_{max} and AUC appeared to be greater than dose proportional at the dose range from 10 to 600 mg, but less than dose proportional from 600 to 1200 mg. This observed dose proportionality may be the result of JNJ 39758979 being the substrate of drug transporters; however, more investigation is needed to support this hypothesis.

The safety data from the preclinical toxicity studies and the phase 1 clinical study suggest that H_4R antagonists should have an overall good safety profile in general. Preclinical toxicity

studies with JNJ 39758979 in both rat and monkey did not reveal any toxicity associated with either the compound or with antagonism of the H_4R. This was true even with chronic daily administration (6 months rat, 9 months monkey). In general no adverse findings were observed at any dose outside of decreases in body weight gain. In the clinic the compound was in general well tolerated up to 1200 mg single dose or 300 mg b.i.d. dosing for 14 days and no safety signals were noted. The only tolerability issue observed was a dose dependent increase in gastrointestinal adverse events that were mainly nausea and vomiting. It is thought that this was a result of a local nonspecific effect in the stomach and tolerability was greatly improved in later clinical studies with an enteric coating (data not shown). Overall, no on-target related safety issues were identified in this phase 1 study, however, a later clinical study (ClinicalTrials.gov Identifier: NCT01497119) did determine that JNJ 39758979 was associated with drug-induced agranulocytosis. The details of this will be disclosed in a separate publication.

In conclusion, JNJ 39758979 is a potent and selective H_4R that exhibited excellent preclinical safety and evidence of a pharmacodynamics effect in humans. Further clinical development of the compound has been terminated due to drug-induced agranulocytosis. Despite the termination of this compound, the data suggests that targeting the H_4R holds promise to deliver safe and effective treatments for a variety of immune-mediated conditions.

Acknowledgments

The authors would like to acknowledge Jeffrey M. Cowden, Jason P. Riley, Patricia McGovern and Paku Desai for technical support.

Authorship Contributions

Participated in research design: Thurmond, Chen, Dunford, Greenspan, Karlsson, La, Ward, Xu

Conducted experiments: Dunford, Greenspan, Xu

Performed data analysis: Thurmond, Chen, Dunford, Greenspan, La, Ward, Xu

Wrote or contributed to the writing of the manuscript: Thurmond, Chen, Dunford, Greenspan, Karlsson, La, Ward, Xu

References

Ballerini C, Aldinucci A, Luccarini I, Galante A, Manuelli C, Blandina P, Katebe M, Chazot PL, Masini E and Passani MB (2013) Antagonism of histamine H4 receptors exacerbates clinical and pathological signs of experimental autoimmune encephalomyelitis. *British Journal of Pharmacology* **170**:67-77.

Cowden JM, Riley JP, Ma JY, Thurmond RL and Dunford PJ (2010a) Histamine H4 receptor antagonism diminishes existing airway inflammation and dysfunction via modulation of Th2 cytokines. *Respiratory Research* **11**:86.

Cowden JM, Yu F, Banie H, Farahani M, Ling P, Nguyen S, Riley JP, Zhang M, Zhu J, Dunford PJ and Thurmond RL (2014) The histamine H4 receptor mediates inflammation and Th17 responses in preclinical models of arthritis. *Annals of the Rheumatic Diseases* **73**:600-608.

Cowden JM, Zhang M, Dunford PJ and Thurmond RL (2010b) The Histamine H_4 Receptor Mediates Inflammation and Pruritus in Th2-Dependent Dermal Inflammation. *Journal of Investigative Dermatology* **130**:1023-1033.

del Rio R, Noubade R, Saligrama N, Wall EH, Krementsov DN, Poynter ME, Zachary JF, Thurmond RL and Teuscher C (2012) Histamine H4 Receptor Optimizes T Regulatory Cell Frequency and Facilitates Anti-Inflammatory Responses within the Central Nervous System. *Journal of Immunology* **188**:541-547.

Dunford PJ, O'Donnell N, Riley JP, Williams KN, Karlsson L and Thurmond RL (2006) The histamine H_4 receptor mediates allergic airway inflammation by regulating the activation of CD4+ T cells. *Journal of Immunology* **176**:7062-7070.

Dunford PJ, Williams KN, Desai PJ, Karlsson L, McQueen D and Thurmond RL (2007) Histamine H_4 receptor antagonists are superior to traditional antihistamines in the attenuation of experimental pruritus. *Journal of Allergy and Clinical Immunology* **119**:176-183.

Gao Y, Davies SP, Augustin M, Woodward A, Patel UA, Kovelman R and Harvey KJ (2013) A broad activity screen in support of a chemogenomic map for kinase signalling research and drug discovery. *Biochemical Journal* **451**:313-328.

Ling P, Ngo K, Nguyen S, Thurmond RL, Edwards JP, Karlsson L and Fung-Leung W-P (2004) Histamine H_4 receptor mediates eosinophil chemotaxis with cell shape change and adhesion molecule upregulation. *British Journal of Pharmacology* **142**:161-171.

Matsushita A, Seike M, Okawa H, Kadawaki Y and Ohtsu H (2012) Advantages of histamine H4 receptor antagonist usage with H1 receptor antagonist for the treatment of murine allergic contact dermatitis. *Exp Dermatol* **21**:714-715.

Mowbray CE, Bell AS, Clarke NP, Collins M, Jones RM, Lane CAL, Liu WL, Newman SD, Paradowski M, Schenck EJ, Selby MD, Swain NA and Williams DH (2011) Challenges of drug discovery in novel target space. The discovery and evaluation of PF-3893787: A novel histamine H4 receptor antagonist. *Bioorganic & Medicinal Chemistry Letters* **21**:6596-6602.

Nent E, Frommholz D, Gajda M, Braeuer R and Illges H (2013) Histamine 4 receptor plays an important role in auto-antibody-induced arthritis. *International Immunology* **25**:437-443.

Ohsawa Y and Hirasawa N (2012) The antagonism of histamine H1 and H4 receptors ameliorates chronic allergic dermatitis via anti-pruritic and anti-inflammatory effects in NC/Nga mice. *Allergy* **67**:1014-1022.

Rossbach K, Nassenstein C, Gschwandtner M, Schnell D, Sander K, Seifert R, Stark H, Kietzmann M and Baeumer W (2011) Histamine H1, H3 and H4 receptors are involved in pruritus. *Neuroscience* **190**:89-102.

Salcedo C, Pontes C and Merlos M (2013) Is the H4 receptor a new drug target for allergies and asthma? *Front. Biosci., Elite Ed.* **E5**:178-187.

Savall BM, Chavez F, Tays K, Dunford P, Cowden J, Hack MD, Wolin R, Thurmond RL and Edwards JP (2014) Discovery and SAR of 6-Alkyl-2,4-diaminopyrimidines as H4 Receptor Antagonists. *Journal of Medicinal Chemistry* **Accepted**:DOI: 10.1021/jm401727m.

Shin N, Covington M, Bian D, Zhuo J, Bowman K, Li Y, Soloviev M, Qian D-Q, Feldman P, Leffet L, He X, Wang KH, Krug K, Bell D, Czerniak P, Hu Z, Zhao H, Zhang J, Yeleswaram S, Yao W, Newton R and Scherle P (2012) INCB38579, a novel and potent histamine H4 receptor small molecule antagonist with anti-inflammatory pain and anti-pruritic functions. *European Journal of Pharmacology* **675**:47-56.

Somma T, Cinci L, Formicola G, Pini A, Thurmond R, Ennis M, Bani D and Masini E (2013) A selective antagonist of histamine H4 receptors prevents antigen-induced airway inflammation and bronchoconstriction in guinea pigs: involvement of lipocortin-1. *British Journal of Pharmacology* **170**:200-213.

Suwa E, Yamaura K, Oda M, Namiki T and Ueno K (2011) Histamine H4 receptor antagonist reduces dermal inflammation and pruritus in a hapten-induced experimental model. *European Journal of Pharmacology* **667**:383-388.

Thurmond RL, Desai PJ, Dunford PJ, Fung-Leung W-P, Hofstra CL, Jiang W, Nguyen S, Riley JP, Sun S, Williams KN, Edwards JP and Karlsson L (2004) A potent and selective

histamine H_4 receptor antagonist with anti-inflammatory properties. *Journal of Pharmacology and Experimental Therapeutics* **309**:404-413.

Varga C, Horvath K, Berko A, Thurmond RL, Dunford PJ and Whittle BJR (2005) Inhibitory effects of histamine H_4 receptor antagonists on experimental colitis in the rat. *European Journal of Pharmacology* **522**:130-138.

Yamaura K, Oda M, Suwa E, Suzuki M, Sato H and Ueno K (2009) Expression of histamine H4 receptor in human epidermal tissues and attenuation of experimental pruritus using H4 receptor antagonist. *Journal of Toxicological Sciences* **34**:427-431.

Yu F, Wolin RL, Wei J, Desai PJ, McGovern PM, Dunford PJ, Karlsson L and Thurmond RL (2010) Pharmacological characterization of oxime agonists of the histamine H4 receptor. *Journal of Receptor, Ligand and Channel Research* **3**:37-49.

Footnotes

[1]Current Address: Novo Nordisk A/S, Novo Nordisk Park, DK-2760 Måløv

Figure legends

Figure 1. The structure of JNJ 39758979

Figure 2. The effects of JNJ 39758979 on histamine-induced eosinophil shape change. (A) Human polymorphonuclear leukocytes were stimulated with various concentrations of histamine in addition to 0 μM (o), 0.03 μM (▲), 0.1 μM (■) or 0.3 μM (●) JNJ 39758979. After 5 min the percent increase in forward scatter (FSC) was measured by flow cytometry. The mean (n=2) and SEM is given. (B) Human blood was incubated with various concentrations of JNJ 39758979 prior to stimulation with 300 nM histamine. The geometric mean (four replicates from four different donors) of the forward scattering (FSC GeoMean) was measured by flow cytometry. Error bars represent SEM. Statistical significance was calculated between untreated and non-manipulated samples (unt), those processed without histamine (base) and samples treated with histamine with or without JNJ 39758979 using a Student's t-test and † indicates $p<0.05$ relative to untreated samples. Statistical significance between each JNJ 39758979 group and vehicle group (0 JNJ 39758979) was assessed by a one-way ANOVA with post-hoc Dunnett's test. *$p < 0.05$, **$p < 0.01$, ***$p < 0.001$.

Figure 3. (A) Female BALB/c mice (n = 10 per group) were sensitized to ovalbumin i.p. on Days 0 and 14 before repeat aerosol exposure to ovalbumin on Day 21 through 24. Vehicle (20% hydroxypropyl-β-cyclodextran), JNJ 39758979 or JNJ 77777120 (20 mg/kg) were administered orally 20 min prior to each challenge. Some mice (n=5) were sensitized with ovalbumin, but challenged with phosphate-buffered saline (PBS) only. The total number of cells and a differential cell count were calculated from bronchoalveolar lavage fluid collected 24 h after the

final challenge. (B) Female Balb/c mice (n = 8 mice per group) were sensitized to fluorescein isothiocyanate on days 0 and 1 and then challenged on day six by application of fluorescein isothiocyanate to one ear. On day seven the difference in ear thickness between the challenged and unchallenged ear was measured with calipers. Vehicle (20% hydroxypropyl-β-cyclodextran), JNJ 39758979 or JNJ 28307474 (50 mg/kg) were administered orally 20 min prior and 4 h after fluorescein isothiocyanate application. For both panels statistical significance between each compound treated group and vehicle was assessed by a one-way ANOVA with post-hoc Dunnett's test. *$p < 0.05$, **$p < 0.01$, ***$p < 0.001$.

Figure 4. Plasma concentration of JNJ 39758979 (mean ± SD) at various time point after a single oral dose in humans. Doses were 10 mg (■), 30 mg (●), 100 mg (□), 300 mg (♦), 600 mg (▼) and 1200 mg (◊).

Figure 5. Plasma concentration of JNJ 39758979 (mean ± SD) at various time point after oral doses on days 1, 7 and 14 in the multiple dose portion of the clinical study. Doses were 30 mg (●), 100 mg (□), 300 mg males (♦), 300 mg females (o) and 300 mg b.i.d. (▼).

Figure 6. Histamine-induced eosinophil shape change assessed during the human clinical study. Blood was stimulated with 0.3 μM histamine for 10 min and then the forward scattering was assessed by flow cytometry. The percent change in the geometric mean of the forward scatter compared to samples where no histamine was added is plotted as box-and-whisker plots indicating the maximum and minimum response. (A) Data from single ascending portion of the clinical study. Data were collected 1 day prior to dosing (-24 h) and at several time point after

dosing. (B) Data from the multiple ascending dose portion of the clinical study. Data were collected 1 day prior to dosing on day 1 (-24 h) and at several time point after dosing on day 14. The data from the female cohort is indicated by F. All other data is from males. Statistical comparison of treated groups to the placebo group was assessed by a one-way ANOVA with post-hoc Dunnett's test. *$p < 0.05$, **$p < 0.01$, ***$p < 0.001$.

JPET Fast Forward. Published on February 18, 2014 as DOI: 10.1124/jpet.113.211714
This article has not been copyedited and formatted. The final version may differ from this version.

Tables

Table 1: K_i, EC_{50}, and pA_2 Values for JNJ-39758979 at Histamine Receptors From Various Species

Receptor	Species	K_i (nM)[a]	EC_{50} (μM)[b]	pA_2[a,b]
H_4	Human	12.5 ± 2.6	>10	7.9 ± 0.1
H_4	Mouse	5.3 ± 0.4	>10	8.3 ± 0.2
H_4	Rat	188 ± 61	>10	7.2 ± 0.2
H_4	Monkey	25 ± 1	>10	7.5 ± 0.1
H_4	Guinea pig	306 ± 23	ND	ND
H_4	Dog	>10,000	ND	ND
H_3	Human	1043 ± 348	ND	ND
H_3	Mouse	202 ± 29	ND	ND
H_3	Rat	258 ± 26	ND	ND
H_2	Human	>1000	ND	ND
H_1	Human	>1000	ND	ND
H_1	Mouse	6800 ± 1800	ND	ND
H_1	Monkey	>10,000	ND	ND

[a] Data given as ± standard error of the mean if the assay was run at least 2 times
[b] ND indicates not determined

JPET Fast Forward. Published on February 18, 2014 as DOI: 10.1124/jpet.113.211714
This article has not been copyedited and formatted. The final version may differ from this version.

Table 2: Treatment-Emergent Adverse events with an Incidence of >1 in Treatment Groups after a Single Oral Dose of JNJ-39758979

		---------- JNJ-39758979 ----------					
	Placebo (N = 18) n (%)	10 mg (N = 6) n (%)	30 mg (N = 5) n (%)	100 mg (N = 6) n (%)	300 mg (N = 6) n (%)	600 mg (N = 6) n (%)	1200 mg (N = 6) n (%)
Diarrhea	2 (11)	0	0	0	0	4 (67)	5 (83)
Nausea	2 (11)	0	0	0	2 (33)	2 (33)	4 (67)
Vomiting	1 (6)	0	0	0	0	0	4 (67)
Abdominal pain	2 (11)	0	0	0	0	1 (17)	1 (17)
Headache	2 (11)	1 (17)	1 (20)	0	0	2 (33)	0

JPET Fast Forward. Published on February 18, 2014 as DOI: 10.1124/jpet.113.211714
This article has not been copyedited and formatted. The final version may differ from this version.

Table 3: Treatment-Emergent Adverse events with an Incidence of >1 in Treatment Groups after 14 Days of Oral Dosing of JNJ-39758979

		JNJ-39758979				
	Placebo (N = 15) n (%)	30 mg QD (N = 6) n (%)	100 mg QD (N = 5) n (%)	300 mg QD (N = 6) n (%)	300 mg BID (N = 6) n (%)	300 mg QD Female (N = 6) n (%)
Abnormal feces	4 (27)	0	4 (80)	2 (33)	4 (67)	2 (33)
Nausea	2 (13)	0	0	2 (33)	1 (17)	6 (100)
Abdominal pain	2 (14)	1 (17)	0	0	1 (17)	1 (17)
Vomiting	0	0	0	1 (17)	0	1 (17)
Headache	4 (27)	2 (33)	2 (40)	1 (17)	1 (17)	3 (50)
Rash	0	0	0	0	0	2 (33)
Influenza like illness	0	0	1 (20)	0	0	1 (2)
Malaise	0	0	0	0	1 (17)	1 (2)
Epistaxis	1 (7)	1 (17)	0	0	0	2 (5)
Oropharyngeal pain	0	1 (17)	0	0	0	1 (2)
Oral herpes	0	1 (17)	0	0	0	1 (2)

JPET Fast Forward. Published on February 18, 2014 as DOI: 10.1124/jpet.113.211714
This article has not been copyedited and formatted. The final version may differ from this version.

Figure 1

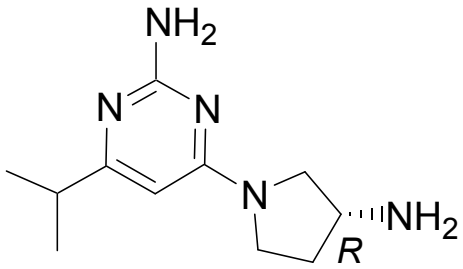

JPET Fast Forward. Published on February 18, 2014 as DOI: 10.1124/jpet.113.211714
This article has not been copyedited and formatted. The final version may differ from this version.

Figure 2

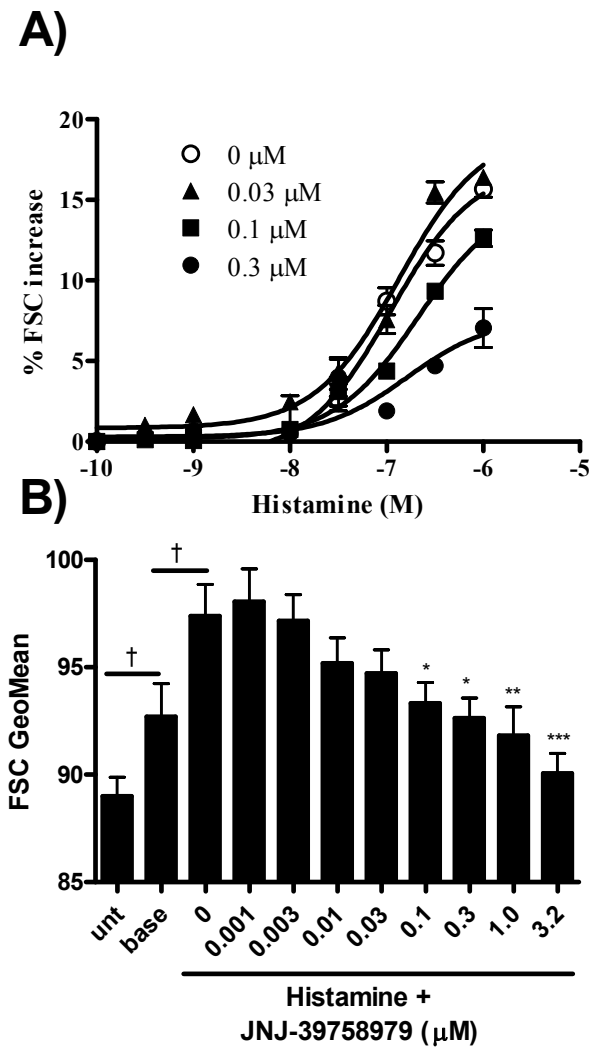

JPET Fast Forward. Published on February 18, 2014 as DOI: 10.1124/jpet.113.211714
This article has not been copyedited and formatted. The final version may differ from this version.

Figure 3

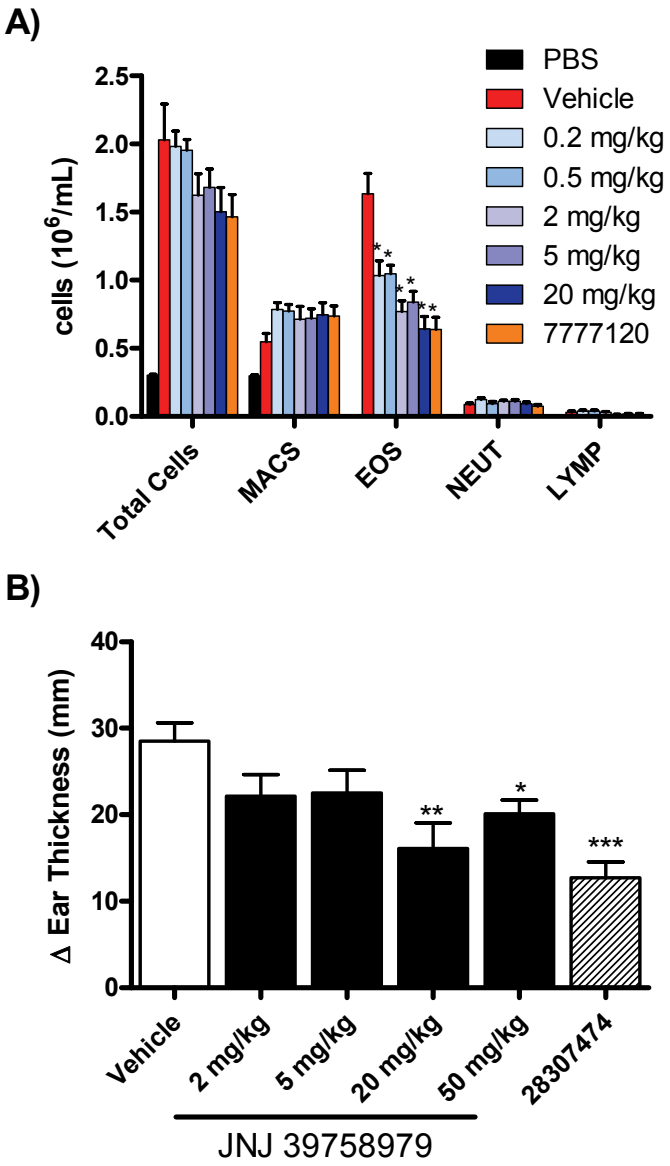

JPET Fast Forward. Published on February 18, 2014 as DOI: 10.1124/jpet.113.211714
This article has not been copyedited and formatted. The final version may differ from this version.

Figure 4

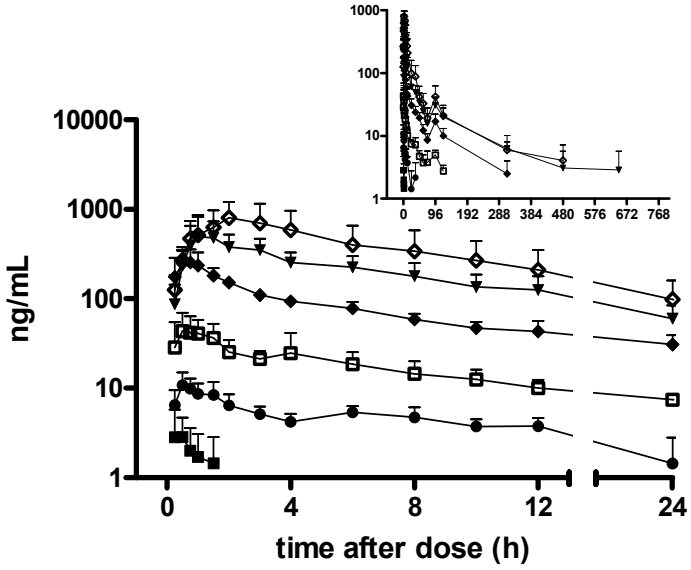

JPET Fast Forward. Published on February 18, 2014 as DOI: 10.1124/jpet.113.211714
This article has not been copyedited and formatted. The final version may differ from this version.

Figure 5

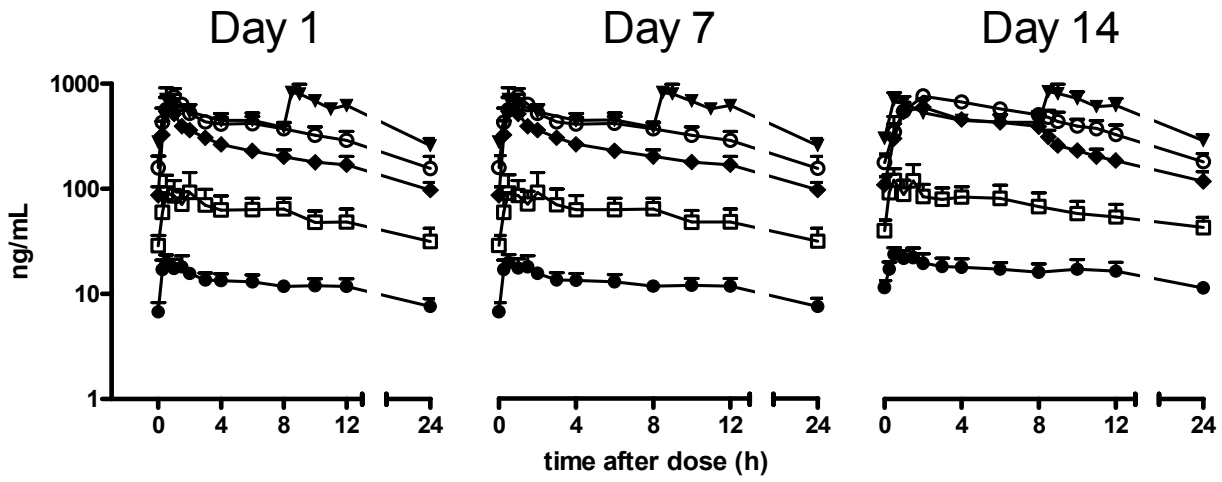

JPET Fast Forward. Published on February 18, 2014 as DOI: 10.1124/jpet.113.211714
This article has not been copyedited and formatted. The final version may differ from this version.

Figure 6

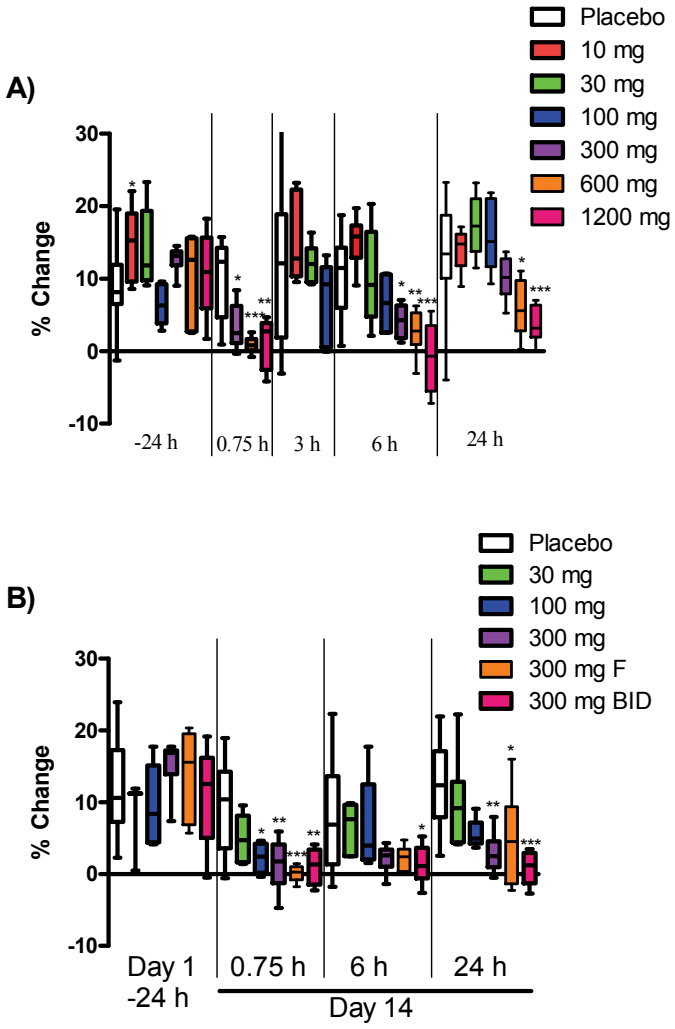

Supplemental Data

Clinical and Preclinical Characterization of the Histamine H_4 Receptor Antagonist JNJ 39758979

Robin L. Thurmond, Bin Chen, Paul J. Dunford, Andrew J. Greenspan, Lars Karlsson, David La, Peter Ward and Xie L Xu

Journal of Pharmacology and Experimental Therapeutics

Supplemental Tables

Table S1: Selectivity of JNJ 39758979 (- indicates <10% inhibition). Assays where human targets are used are indicated by h.

Target	% Inhibition at 1 μM	Target	% Inhibition at 1 μM
A1 (h)	-	M3 (h)	64
A2A (h)	-	NK2 (h)	-
A3 (h)	-	NK3 (h)	-
alpha 1 (non-selective)	-	Y1 (h)	-
alpha 2 (non-selective)	18	Y2 (h)	-
beta 1 (h)	-	NT1 (h) (NTS1)	-
NE transporter (h)	10	delta (h)	-
AT1 (h)		kappa (h)	-
BZD (central)	-	mu (h)	-
B2 (h)	-	ORL1 (h)	-
CCKA (h) (CCK1)	-	5-HT1A (h)	-
D1 (h)	-	5-HT1B	-
D2 (h)	-	5-HT2A (h)	-
DA transporter (h)	18	5-HT3 (h)	-
ETA (h)	15	5-HT5A (h) (5-ht5a)	-
GABA (non-selective)	-	5-HT6 (h) (5-ht6)	-
GAL2 (h)	-	5-HT7 (h)	-
IL-8B (h) (CXCR2)	-	sst (non-selective)	-
CCR1 (h)	-	VIP1 (h) (VPAC1)	-
H_1 (h)	-	V1A (h)	-
H_2 (h)	-	Ca2+ channel	-
MC4 (h)	-	K+V channel	-
MT1	-	SK+Ca channel	-
M1 (h)	19	Na+ channel (site 2)	-
M2 (h)	-	Cl- channel	-

Table S2: Selectivity of JNJ 39758979 against various kinases.

Target	% Inhibition at 10 μM	Target	% Inhibition at 10 μM
Abl(h)	-2	JAK2(h)	-7
ALK(h)	12	JNK1α1(h)	10
AMPK(r)	1	LIMK1(h)	-10
Aurora-A(h)	-14	LKB1(h)	0
Axl(h)	-11	MAPKAP-K2(h)	-11
BTK(h)	-9	Met(h)	-15
CaMKI(h)	3	MLK1(h)	6
CaMKII(r)	-18	MSK1(h)	6
CDK2/cyclinA(h)	-3	MSSK1(h)	-1
CHK1(h)	-18	MuSK(h)	-9
CHK2(h)	4	NEK2(h)	-10
CK1δ(h)	1	p70S6K(h)	8
CK2(h)	4	PDK1(h)	-4
CLK3(h)	9	Pim-1(h)	3
c-RAF(h)	-5	PKA(h)	-2
CSK(h)	-9	PKBα(h)	-7
cSRC(h)	-5	PKBβ(h)	-5
DAPK1(h)	-3	PKBγ(h)	-3
DCAMKL2(h)	1	PKCα(h)	23
DDR2(h)	-8	PKD2(h)	8
DYRK2(h)	-20	PKG1α(h)	-2
EGFR(h)	2	Plk3(h)	-5
EphA1(h)	-6	Ret(h)	-6
FAK(h)	-1	Ros(h)	6
Fer(h)	-8	SAPK2a(h)	-12
FGFR1(h)	-13	SGK(h)	7
Flt3(h)	-12	STK33(h)	-4
GSK3α(h)	8	Syk(h)	3
GSK3β(h)	0	Tie2(h)	12
IGF-1R(h)	-27	TrkA(h)	13
IKKα(h)	-18	TSSK1(h)	16
IRAK1(h)	-6	WNK2(h)	-5
IRAK4(h)	-5	VRK2(h)	-2

Table S3: Mean (SD) Single Dose Plasma JNJ-39758979 Pharmacokinetic Parameters (Oral Solution, Fasting)

Dose (n)	C_{max} (ng/mL)	T_{max} (h)	AUC_{0-24} (ng•h/mL)	AUC_{0-120} (ng•h/mL)	AUC_{last} (ng•h/mL)	AUC_{0-inf} (ng•h/mL)	AUC_{extrap} (%)	V_d/F (L)	CL/F (L/h)	$t_{1/2}$ (h)
10 mg	4.19	0.50	NC	NC	NC	NC	NC	NC	NC	NC
(n = 5)	(2.08)	(0.25-1.0)								
30 mg	11.5	0.75	97.9[a]	NC	102	NC	NC	NC	NC	NC
(n = 5)	(3.55)	(0.50-1.5)	(22.3)		(44)					
100 mg	55.3	0.88	345	799	979	1,450	31.9	12,600	80.0	126
(n = 6)	(20.5)	(0.25-1.5)	(95)	(177)	(423)	(624)	(8.9)	(4,540)	(31.1)	(60)
300 mg	280	0.75	1,560	3,100	4,550	5,240	14.0	10,500	64.4	127
(n = 6)	(100)	(0.50-1.5)	(277)	(602)	(1,690)	(1,890)	(6.9)	(1,050)	(25.8)	(46)
600 mg	591	1.8	3,930	6,860	10,800	11,800	7.58	12,200	58.2	157
(n = 6)	(274)	(1.0-3.0)	(1,300)	(2,170)	(4,460)	(5,300)	(4.22)	(3,650)	(21.7)	(56)
1200 mg	879	1.8	6,980	11,100	14,900	15,400	3.91	18,400	103	124
(n = 6)	(361)	(0.75-3.0)	(4,210)	(6,230)	(8,110)	(8,160)	(2.08)	(11,400)	(58)	(18)

[a] n = 3

AUC_{0-24} = area under the plasma concentration-time curve from time 0 through 24 hours; AUC_{0-120} = area under the plasma concentration-time curve from time 0 through 120 hours; AUC_{0-inf} = area under the plasma concentration-time curve extrapolated to infinity; AUC_{last} = area under the plasma concentration-time curve from time 0 through the time of last concentration above the lower limit of quantification; AUC_{extrap} (%) = $AUC_{0-t}/AUC_{0-inf} \times 100\%$; CL/F = apparent clearance; C_{max} = maximum concentration; NC = not calculated due to insufficient concentration data above lower limit of quantification for the calculation of pharmacokinetic parameters; SD = standard deviation; $t_{1/2}$ = terminal half-life; T_{max} = time to the maximum concentration; V_d/F = apparent volume of distribution.

Table S4: Mean (SD) Multiple Dose Plasma Pharmacokinetic Parameters of JNJ-39758979 (Oral Solution, Fasting)

	Day 1			Day 7			Day 14									
Dose (n)	T_{max} (h)	C_{max} (ng/mL)	AUC_{0-24} (ng•h/mL)	T_{max} (h)	C_{max} (ng/mL)	AUC_{0-24} (ng•h/mL)	T_{max} (h)	$C_{max(ss)}$ (ng/mL)	$C_{min(ss)}$ (ng/mL)	$C_{avg(ss)}$ (ng/mL)	AUC_{0-24} (ng•h/mL)	FI	AR	$V_{d(ss)}/F$ (L)	CL/F_{ss} (L/h)	$t_{1/2}$ (h)
30 mg QD	1.0	12.9	108	0.75	22.0	277	1.3	25.0	11.5	15.9	381	0.852	3.93	15,600	79.7	134
(n = 6, M)	(0.50-4.0)	(5.1)	(38)	(0.25-1.50)	(3.7)	(41)	(0.50-10)	(4.5)	(1.9)	(2.0)	(48)	(0.203)	(1.45)	(6,100)	(9.3)	(42)
100 mg QD	1.0	62.0	483	2.0	119	1,240	0.50	139	39.9	62.3	1,490	1.58	3.19	19,000	70.6	189
(n = 5, M)	(0.50-4.0)	(31.1)	(140)	(0.5-8.0)	(47)	(350)	(0.25-1.5)	(46)	(10.3)	(15.1)	(361)	(0.53)	(0.83)	(8,960)	(19.4)	(80)
300 mg QD	1.0	383	1,860	0.75	610	4,720	0.75	690	109	225	5,390	2.60	3.00	14,000	56.3	176
(n = 6, M)	(0.50-1.5)	(113)	(449)	(0.50-1.0)	(151)	(513)	(0.50-1.0)	(132)	(20)	(28)	(663)	(0.64)	(0.66)	(4,680)	(6.7)	(70)
300 mg QD	1.0	382	2,120	1.0	758	7,340	1.0	770	179	354	8,490	1.73	4.02	14,900	36.0	296
(n = 6, F)	(1.0-1.5)	(136)	(227)	(1.0-1.5)	(146)	(1,400)	(1.0-1.5)	(53)	(36)	(52)	(1,250)	(0.48)	(0.58)	(2,440)	(5.8)	(84)
300 mg BID AM[a,b]	0.75	370	1,020	0.5	735	3,900	0.75	717	NC	NC	3,910	NC	NC	NC	NC	NC
(n = 6, M)	(0.50-1.0)	(160)	(277)	(0.5-6.0)	(186)	(454)	(0.50-1.0)	(109)			(387)					
300 mg BID PM[a,c]	0.75	524	2,970	0.75	870	7,960	0.5	908	305	506	8,250	1.20	3.17	17,100	49.8	259
(n = 6, M)	(0.50-1.0)	(242)	(756)	(0.50-4.0)	(170)	(828)	(0.5-4.0)	(159)	(22)	(53)	(939)	(0.34)	(0.64)	(3,530)	(5.2)	(93)

[a] For 300 mg BID AM: AUC is calculated AUC_{0-8}. For 300 mg BID PM, AUC is calculated AUC_{8-24}.

[b] Accumulation Ratio for 300 mg BID : $(AUC_{0-8} + AUC_{8-24})_{Day\ 14}$ / $(AUC_{0-8} + AUC_{8-24})_{Day\ 1}$

[c] For 300 mg BID PM: T_{max} is calculated as time after second dose

AM = morning; AR = accumulation ratio; AUC_{0-24} = area under the plasma concentration-time curve from time 0 to 24 hours; BID = twice daily dosing; C_{max} = maximum concentration; $C_{max(ss)}$ = maximum concentration at the steady-state; $C_{min(ss)}$ = minimum concentration at the steady-state; $C_{avg(ss)}$ = average concentration ($AUC_{0-24,day\ 14}/24$); CL/F_{ss} = apparent clearance at steady-state; F = female; FI = fluctuation index at the steady-state ($(C_{max(ss)}C_{min(ss)})/C_{avg(ss)}$); M = male; NC = not calculated; PM = afternoon; QD = once daily dosing; SD = standard deviation; T_{max} = time to the maximum concentration; $t_{1/2}$ = half-life; $V_{d(ss)}/F$ = apparent volume of distribution at the steady-state.

Table S5: Serum protein analyzed in clinical samples by Rules Based Medicine.

Alpha-1 Antitrypsin	**Fibrinogen**	**IL-7**	**TNF-alpha**
Adiponectin	**G-CSF**	**IL-8**	**TNF-beta**
Alpha-2 Macroglobulin	**Growth Hormone**	**Insulin**	**Thrombopoietin**
Alpha-Fetoprotein	**GM-CSF**	**Leptin**	**Thyroid Stimulating Hormone**
Amphiregulin	**Glutathione S-Transferase**	**Lipoprotein (a)**	**VCAM-1**
Apolipoprotein A1	**Haptoglobin**	**Lymphotactin**	**VDBP (Vitamin D Binding Protein)**
Apolipoprotein CIII	**ICAM-1**	**MCP-1**	**VEGF**
Apolipoprotein H	**IFN-gamma**	**MDC**	**von Willebrand Factor**
Beta-2 Microglobulin	**IgA**	**MIP-1alpha**	
Brain-Derived Neurotrophic Factor	**IgE**	**MIP-1beta**	
Complement 3	**IGF-1**	**MMP-2**	
Cancer Antigen 125	**IgM**	**MMP-3**	
Cancer Antigen 19-9	**IL-10**	**MMP-9**	
Calcitonin	**IL-12p40**	**Myeloperoxidase**	
CD40	**IL-12p70**	**Myoglobin**	
CD40 Ligand	**IL-13**	**OSM (Oncostatin M)**	
Carcinoembryonic Antigen	**IL-15**	**PAI-1**	
Creatine Kinase-MB	**IL-16**	**Prostatic Acid Phosphatase**	
C Reactive Protein	**IL-17**	**PAPP-A**	
EGF	**IL-17E**	**Prostate Specific Antigen, Free**	
ENA-78	**IL-18**	**RANTES**	
Endothelin-1	**IL-1alpha**	**Serum Amyloid P**	
EN-RAGE	**IL-1beta**	**Stem Cell Factor**	
Eotaxin	**IL-1ra**	**SGOT**	
Epiregulin	**IL-2**	**SHBG**	
Erythropoietin	**IL-23**	**Thyroxine Binding Globulin**	
Fatty Acid Binding Protein	**IL-3**	**Tissue Factor**	
Factor VII	**IL-4**	**TGF-alpha**	
Ferritin	**IL-5**	**TIMP-1**	
FGF basic	**IL-6**	**TNF RII**	

Table S6: Mean WBC and WBC differentials in rat 6-month study

	Mean Values, x10^3/μL						
Group	WBC	Neut	Lymph	Mono	Eos	Baso	Luc
Males							
0	7.62	1.24	5.89	0.28	0.14	0.01	0.05
25	8.63	1.65	6.47	0.30	0.13	0.02	0.06
50	9.30	1.82	6.88	0.36	0.15	0.02	0.07
100	7.92	1.35	6.14	0.27	0.09	0.01	0.05
200	7.03	1.49	5.20	0.25	0.04	0.01	0.04
Females							
0	4.79	0.68	3.81	0.16	0.10	0.01	0.04
25	4.91	0.55	4.06	0.17	0.09	0.01	0.04
50	5.01	0.61	4.12	0.16	0.08	0.01	0.04
100	5.16	0.66	4.24	0.14	0.07	0.01	0.04
200	4.55	0.70	3.57	0.17	0.06	0.01	0.04

Blood was collected for hematology at study termination from N=20 animals/group.
Abbreviations: WBC, white blood cells; Neut, absolute neutrophils; Lymph, absolute lymphocytes; Mono, absolute monocytes; Eos, absolute eosinophils; Baso, absolute basophils; Luc, absolute large unstained cells.

Table S7: Mean WBC and WBC differentials in monkey 9-month study

	Mean Values, x10^3/μL						
Group	WBC	Neut	Lymph	Mono	Eos	Baso	Luc
Males							
0	10.69	3.31	6.64	0.54	0.13	0.03	0.05
3	11.12	3.66	6.64	0.50	0.25	0.03	0.06
10	9.60	2.79	6.27	0.34	0.13	0.02	0.04
30	8.41	2.48	5.33	0.46	0.09	0.02	0.04
Females							
0	8.05	2.21	5.16	0.35	0.30	0.02	0.02
3	10.59	5.02	4.91	0.47	0.11	0.03	0.04
10	7.06	2.40	4.12	0.34	0.16	0.01	0.03
30	6.22	2.28	3.55	0.29	0.08	0.01	0.02

Blood was collected for hematology at study termination from N=4 animals/group.
Abbreviations: WBC, white blood cells; Neut, absolute neutrophils; Lymph, absolute lymphocytes; Mono, absolute monocytes; Eos, absolute eosinophils; Baso, absolute basophils; Luc, absolute large unstained cells.

Table S8: Bone marrow cytology in monkey 3-month study

	Group			
	Males		Females	
Cell Type	0	30	0	30
Myeloblast	0.0	0.0	0.0	0.2
Promyelocyte	0.4	0.3	0.3	0.6
Myelocyte neutrophil	4.0	3.8	2.3	3.8
Metamyelocyte neutrophil	5.3	5.5	5.4	4.1
Band neutrophil	10.8	12.6	12.0	10.2
Segmented neutrophil	20.9	19.3	18.0	20.5
Eosinophil	1.3	1.7	1.8	1.2
Basophil	0.2	0.1	0.1	0.1
Myeloid mitotic figures	0.3	0.1	0.1	0.2
Total granulocytic cells	43.2	43.4	39.9	40.8
Rubriblast	0.0	0.0	0.0	0.0
Prorubricyte	0.2	0.3	0.2	0.4
Rubricyte - basophilic	4.8	3.3	4.0	6.5
Rubricyte - polychromatophilic	23.8	21.2	20.8	18.4
Metarubricyte	7.3	11.2	10.2	11.0
Erythroid Mitotic Figures	0.6	0.4	0.4	0.3
Total erythroid cells	36.7	36.5	35.6	36.5
Lymphoid	19.9	19.6	24.0	21.9
Monocyte	0.0	0.0	0.0	0.0
Plasma Cell	0.2	0.5	0.5	0.7
Mast Cell	0.0	0.0	0.0	0.0
Myeloid: Erythroid (M:E) ratio	1.2	1.2	1.1	1.1

Bone marrow was collected and smears were prepared at terminal necropsy from 0 and 30 mg/kg/day groups (N=4/group) of a monkey 3-month toxicity study.

Table S9: Incidence of microscopic changes in lymphoid organs in rat 6-month study

	Group			
	Males		Females	
Tissue/Organ	0	200	0	200
Bone marrow	0/20	0/20	0/19	0/20
Lymph node	1/20[1]	2/20[1]	0/19	1/20[1]
Spleen	0/20	2/20[2]	0/19	2/20[2]
Thymus	20/20[3]	18/20[3]	17/19[3]	20/20[3]

[1]Increased sinus histiocytes, pigmented macrophages, intrasinusoidal erythrocytes
[2]Increased hemosiderin
[3]Decreased lymphocytes

Table S10: Incidence of microscopic changes in lymphoid organs in monkey 9-month study

	Group							
	Males				Females			
Tissue/Organ	0	3	10	30	0	3	10	30
Bone marrow, femur	0/4	0/4	1/4[1]	3/4[1]	1/4[1]	1/4[1]	4/4[1]	4/4[1]
Bone marrow, sternum	0/4	0/4	1/4[1]	2/4[1]	0/4	1/4[1]	1/4[1]	2/4[1]
Lymph node	0/4	0/4	0/4	0/4	0/4	0/4	1/4[2]	0/4
Spleen	0/4	0/4	0/4	0/4	0/4	0/4	0/4	0/4
Thymus	0/4	0/4	0/4	0/4	0/4	0/4	1/4[3]	0/4

[1]Lymphoid follicles
[2]Mineralization and necrosis in mesenteric lymph node
[3]Involution

Table S11: Mean WBC and WBC differentials in C57BL/6 wild-type and H4R-deficient mice

	Mean Values, $x10^3/\mu L$						
Group	WBC	Neut	Lymph	Mono	Eos	Baso	Luc
Juvenile animals							
Male WT	6.76	0.29	6.16	0.14	0.04	0.02	0.09
Male KO	3.27	0.14	3.03	0.06	0.01	0.00	0.02
Female WT	3.33	0.16	3.06	0.06	0.02	0.00	0.02
Female KO	3.73	0.19	3.41	0.07	0.03	0.01	0.02
Mature animals							
Male WT	6.98	0.77	5.88	0.07	0.16	0.01	0.10
Male KO	4.55	1.06	3.30	0.05	0.08	0.01	0.05
Female WT	3.52	0.56	2.87	0.02	0.05	0.01	0.02
Female KO	3.87	0.61	3.13	0.02	0.09	0.00	0.02

Blood was collected from C57BL/6 wild-type and H4R-deficient mice. Juvenile and mature animals were evaluated (N=4-5/group). Abbreviations: WBC, white blood cells; Neut, absolute neutrophils; Lymph, absolute lymphocytes; Mono, absolute monocytes; Eos, absolute eosinophils; Baso, absolute basophils; Luc, absolute large unstained cells.

Table S12: Bone marrow cytology in juvenile C57BL/6 wild-type and H4R-deficient mice

	Group			
	Males		Females	
Cell Type	Wild-type	Knock-out	Wild-type	Knock-out
Myeloblast	0.00	0.00	0.00	0.00
Promyelocyte	0.33	0.39	0.08	0.51
Myelocyte neutrophil	1.21	0.59	1.31	1.10
Metamyelocyte neutrophil	3.99	3.24	2.29	2.92
Band neutrophil	8.40	7.60	7.37	6.17
Segmented neutrophil	22.22	21.39	17.09	18.64
Eosinophil	2.92	3.03	2.87	4.89
Basophil	0.00	0.20	0.00	0.00
Myeloid mitotic figures	0.16	0.16	0.08	0.21
Total granulocytic cells	39.25	36.40	31.09	34.45
Rubriblast	0.00	0.00	0.00	0.00
Prorubricyte	0.79	0.26	0.71	0.46
Rubricyte – basophilic	9.05	7.31	8.24	9.80
Rubricyte - polychromatophilic	15.43	17.66	14.55	14.31
Metarubricyte	8.26	7.15	6.31	5.26
Erythroid mitotic figures	0.88	0.84	0.64	0.84
Total erythroid cells	34.41	33.22	30.45	30.67
Lymphoid	26.30	30.38	38.26	34.80
Monocyte	0.00	0.00	0.00	0.00
Plasma Cell	0.04	0.00	0.20	0.09
Mast Cell	0.00	0.00	0.00	0.00
Myeloid: Erythroid (M:E) ratio	1.14	1.10	1.02	1.22

Bone marrow was collected and smears were prepared from juvenile animals (N=4-5/group)

Table S13: Bone marrow cytology in mature C57BL/6 wild-type and H4R-deficient mice

	Group			
	Males		Females	
Cell Type	Wild-type	Knock-out	Wild-type	Knock-out
Myeloblast	0.00	0.04	0.00	0.00
Promyelocyte	0.30	0.24	0.39	0.23
Myelocyte neutrophil	0.67	0.78	1.14	1.05
Metamyelocyte neutrophil	2.99	3.28	2.89	2.58
Band neutrophil	10.39	11.16	10.16	9.15
Segmented neutrophil	35.81	42.74	24.55	24.01
Eosinophil	3.54	3.81	4.60	4.15
Basophil	0.00	0.00	0.00	0.00
Myeloid mitotic figures	0.16	0.20	0.15	0.16
Total granulocytic cells	53.86	62.27	43.89	41.35
Rubriblast	0.00	0.00	0.00	0.00
Prorubricyte	0.24	0.08	0.31	0.65
Rubricyte – basophilic	5.50	4.19	7.83	7.34
Rubricyte - polychromatophilic	12.15	9.29	13.75	15.12
Metarubricyte	6.83	5.00	6.85	6.61
Erythroid mitotic figures	0.15	0.33	1.04	0.54
Total erythroid cells	24.87	18.89	29.78	30.26
Lymphoid	20.67	18.72	25.86	27.88
Monocyte	0.00	0.00	0.00	0.00
Plasma Cell	0.61	0.12	0.47	0.51
Mast Cell	0.00	0.00	0.00	0.00
Myeloid: Erythroid (M:E) ratio	2.44	3.95	1.51	1.42

Bone marrow was collected and smears were prepared from mature animals (N=4-5/group)